

Why Is the Concerted (2+2) Mechanism of the Reactions of SO₃ with Alkenes Favored over the (3+2) Mechanism? Density Functional and Correlated ab Initio Calculations and a Frontier MO Analysis

Jan Haller, Brett R. Beno, and K. N. Houk*

Contribution from the Department of Chemistry and Biochemistry, University of California, Los Angeles, Los Angeles, California 90095-1569

Received December 15, 1997

Abstract: The (2+2) cycloadditions of SO₃ to ethene, propene, and 2-methylpropene were investigated with Hartree–Fock, MP2, QCISD(T), and hybrid Hartree–Fock/density functional theory (HF-DFT) methods. Experimental data support a (2+2) mechanism for these reactions. The thermally allowed (3+2) cycloadditions of SO₃ to ethene and propene were also examined. With the exception of MP2 calculations, all levels of theory predict that SO₃ reacts by a concerted (2+2) pathway. The transition structure has considerable zwitterionic character, and there is a strong preference for Markovnikov addition. The rearrangements of sulfites to sulfoxones are disfavored. The origin of the large preference for the normally forbidden (2+2) process is attributed to frontier orbital interactions, and is contrasted to the (3+2) cycloaddition mechanism favored by OsO₄.

Introduction

The reaction of SO₃ with alkenes was discovered in 1838¹ and is used commercially for the production of surfactants.² The industrial-scale reaction involves liquid SO₃. In contrast, mechanistic studies^{3–6} are usually performed with dichloromethane as the solvent and the less reactive SO₃/dioxane complex⁷ as a reagent. The initial products of reactions of simple alkenes with SO₃ are the β -sulfones (**2**, Figure 1), which are thermally unstable, and undergo isomerization to γ - and δ -sulfones and alkenesulfonic acids.^{3–5} The reaction is a thermally induced (2+2) addition.^{4,5a,6} Because regioisomers are formed according to Markovnikov's rule,^{4a,5a} the mechanism of the reaction has been proposed to involve a zwitterionic

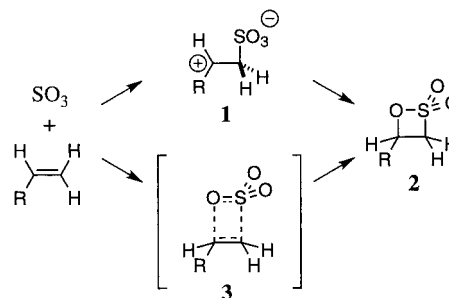


Figure 1. Two possible reaction pathways leading to sulfone **2**.

intermediate (**1**). However, strict stereospecificity, with retention of configuration, is observed: *trans*-sulfones are formed from *E*-alkenes, and *cis*-sulfones from *Z*-alkenes, and this is the case whether SO₃ or the SO₃/dioxane complex is used as the sulfonating reagent.^{5a,6} A long-lived zwitterionic intermediate is therefore unlikely.⁶ Instead, either the ring closure must be faster than rotation about the C–C bond, or the reaction must occur via a concerted (2+2) mechanism (**3**) despite the fact that the (2+2) pathway is forbidden according to orbital symmetry selection rules. The small difference between the rates of reaction of terminal and gem-disubstituted alkenes,⁴ and internal and terminal alkenes,^{5c} implies a concerted mechanism rather than a stepwise zwitterionic mechanism. NMR evidence also supports this view.^{4,5a}

To elucidate the mechanistic details for this reaction, we have performed ab initio and density functional (DFT) calculations on the (2+2) cycloaddition pathway. For purposes of comparison, and to test whether HF, DFT, or MP2 methods incorrectly favor (3+2) over (2+2) cycloaddition mechanisms, a (3+2) mechanism for the cycloadditions of SO₃ to alkenes was examined as well. The route by which (2+2) and (3+2) adducts are interconverted has also been examined. The mechanism of sulfonation is compared to that of alkene

- (1) Regnault, V. *Ann.* **1838**, *25*, 32.
 (2) Gilbert, E. E. *Sulfonation and Related Reactions*; Interscience Publishers: New York, 1965; pp 42–53.
 (3) (a) Bordwell, F. G.; Suter, C. M.; Webber, A. J. *J. Am. Chem. Soc.* **1945**, *67*, 828. (b) Bordwell, F. G.; Rondstedt, C. S., Jr. *J. Am. Chem. Soc.* **1948**, *70*, 2429. (c) Bordwell, F. G.; Peterson, M. L. *J. Am. Chem. Soc.* **1954**, *76*, 3952. (d) Bordwell, F. G.; Peterson, M. L. *J. Am. Chem. Soc.* **1954**, *76*, 3957. (e) Bordwell, F. G.; Peterson, M. L. *J. Am. Chem. Soc.* **1959**, *81*, 2000.
 (4) (a) Roberts, D. W.; Williams, D. L.; Bethell, D. *J. Chem. Soc., Perkin Trans. 2* **1985**, 389. (b) Roberts, D. W.; Jackson, P. S.; Saul, C. D.; Clemett, C. J. *Tetrahedron Lett.* **1987**, *28*, 3386.
 (5) (a) Bakker, B. H.; Cerfontain, H. *Tetrahedron Lett.* **1987**, *28*, 1699. (b) Bakker, B. H.; Cerfontain, H. *Tetrahedron Lett.* **1987**, *28*, 1703. (c) Bakker, B. H.; Cerfontain, H. *Tetrahedron Lett.* **1989**, *30*, 5451. (d) Bakker, B. H.; Schonk, R. M.; Cerfontain, H. *Recl. Trav. Chim. Pays-Bas* **1990**, *109*, 485. (e) Schonk, R. M.; Bakker, B. H.; Cerfontain, H. *Recl. Trav. Chim. Pays-Bas* **1992**, *111*, 49. (f) Schonk, R. M.; Bakker, B. H.; Cerfontain, H. *Recl. Trav. Chim. Pays-Bas* **1993**, *112*, 201. (g) Schonk, R. M.; Meijer, C. W.; Bakker, B. H.; Zöllner, S.; Cerfontain, H.; de Meijere, A. *Recl. Trav. Chim. Pays-Bas* **1993**, *112*, 457. (h) Cerfontain, H.; Kramer, J. B.; Schonk, R. M.; Bakker, B. H. *Recl. Trav. Chim. Pays-Bas* **1995**, *114*, 410.
 (6) Nagayama, M.; Okumura, O.; Noda, S.; Mandai, H.; Mori, A. *Bull. Chem. Soc. Jpn.* **1974**, *47*, 2158.
 (7) Suter, C. M.; Evans, P. B.; Kiefer, J. M. *J. Am. Chem. Soc.* **1938**, *60*, 538.

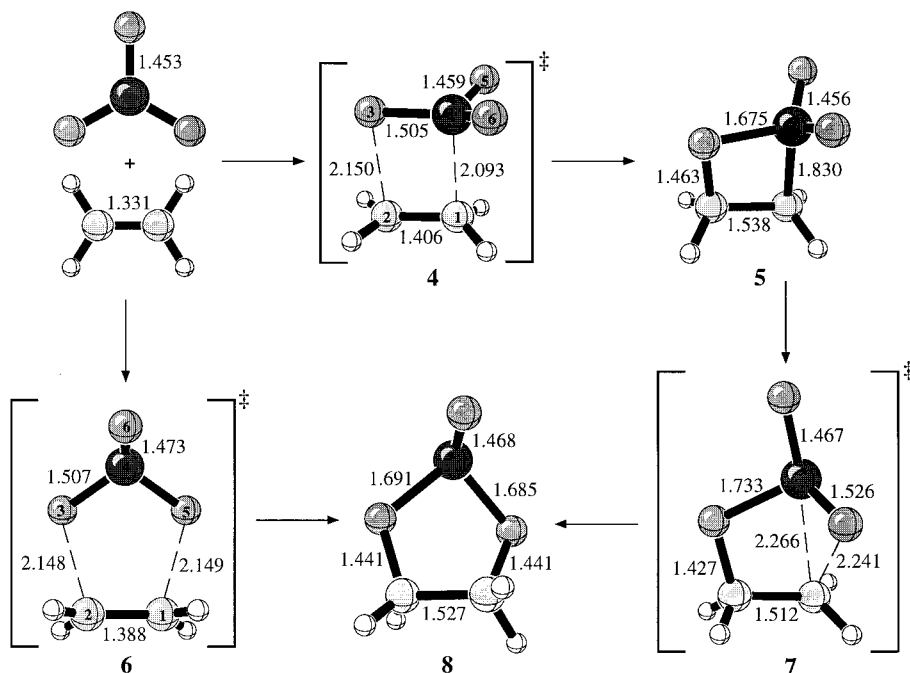


Figure 2. Summary of the reaction pathways and B3LYP/6-31G* geometries for the cycloaddition of SO₃ to ethene. All bond lengths are in Å.

osmylation. Both a concerted (3+2) path⁸ and a stepwise mechanism involving a (2+2) cycloaddition⁹ have been proposed for the osmylation, which gives a cyclic osmate ester product. Recent calculations and experimental isotope effects strongly favor the concerted (3+2) pathway for osmylation.¹⁰ Since the SO₃ reaction strongly favors the (2+2) process experimentally, we have compared these reactions to understand why entirely different reaction mechanisms are chosen by these apparently similar reagents.

Computational Methodology

Calculations were carried out with the Gaussian 94 suite of programs.¹¹ Geometries of stationary points were optimized at the Hartree–Fock (RHF) or density functional theory (DFT, B3LYP)¹² levels of theory using the 6-31G* basis set. All stationary points were confirmed to be minima or first-order saddle points on their respective potential energy hypersurfaces with harmonic frequency calculations. Single-point energies were determined at the RHF and QCISD(T) levels of theory using the 6-311+G* and 6-31G* basis sets, respectively, and RHF/6-31G* optimized geometries. Unrestricted Hartree–Fock (UHF) and B3LYP (UB3LYP) single-point energies were calculated for the RHF and B3LYP structures, respectively, to test for open-shell character. The effect of solvent on relative energies was evaluated

(8) Criegee, R. *Justus Liebigs Ann. Chem.* **1936**, 522, 75.

(9) (a) Hentges, S. G.; Sharpless, K. B. *J. Am. Chem. Soc.* **1980**, *102*, 4263. (b) Sharpless, K. B.; Teranishi, A. Y.; Bäckwall, J.-E. *J. Am. Chem. Soc.* **1977**, *99*, 3120.

(10) (a) Del Monte, A. J.; Haller, J.; Houk, K. N.; Sharpless, K. B.; Singleton, D. A.; Strassner, T.; Thomas, A. A. *J. Am. Chem. Soc.* **1997**, *119*, 9907. (b) Pidun, E.; Boehme, C.; Frenking, G. *Angew. Chem., Int. Ed. Engl.* **1996**, *35*, 2817. (c) Dapprich, S.; Ujaque, G.; Maseras, F.; Lledós, A.; Musaev, D. G.; Morokuma, K. *J. Am. Chem. Soc.* **1996**, *118*, 11660. (d) Torrent, M.; Deng, L.; Duran, M.; Sola, M.; Ziegler, T. *Organometallics* **1997**, *16*, 13.

(11) Gaussian 94 (Revision C.2), Frisch, M. J.; Trucks, G. W.; Schlegel, H. B.; Gill, P. M. W.; Johnson, B. G.; Robb, M. A.; Cheeseman, J. R.; Keith, T.; Petersson, G. A.; Montgomery, J. A.; Raghavachari, K.; Al-Laham, M. A.; Zakrzewski, V. G.; Ortiz, J. V.; Foresman, J. B.; Cioslowski, J.; Stefanov, B. B.; Nanayakkara, A.; Challacombe, M.; Peng, C. Y.; Ayala, P. Y.; Chen, W.; Wong, M. W.; Andres, J. L.; Replogle, E. S.; Gomperts, R.; Martin, R. L.; Fox, D. J.; Binkley, J. S.; Defrees, D. J.; Baker, J.; Stewart, J. P.; Head-Gordon, M.; Gonzalez, C.; Pople, J. A.; Gaussian, Inc.: Pittsburgh, PA, 1995.

(12) (a) Becke, A. D. *J. Chem. Phys.* **1993**, *98*, 5648. (b) Lee, C.; Yang, W.; Parr, R. G. *Phys. Rev. B* **1988**, *37*, 785.

with single-point B3LYP calculations utilizing the self-consistent reaction field (SCRF),¹³ self-consistent isodensity point charge model (SCIPCM),¹³ and the B3LYP/6-31G* optimized structures. The dielectric constant of dichloromethane, $\epsilon = 9.08$, was used in the continuum solvation model calculations. The orbital plots shown in Figure 3 were generated with Spartan¹⁴ using an RHF/6-31G* wavefunction for SO₃ and a wavefunction for OsO₄ that utilized the RHF/6-31G* basis set for the oxygen atoms, and an effective core potential and (341/321/21) basis set for the core and valence electrons of osmium,¹⁵ respectively. The 6-31G* basis set for these single points included five pure rather than six Cartesian d-functions.

Results and Discussion

SO₃ Plus Ethene. The (2+2) and (3+2) cycloaddition transition structures (**4** and **6**) for the reaction of SO₃ with ethene, the transition structure (**7**) for the rearrangement of the sultone (**5**) to the sulfite (**8**), and the structures of the reactants and products were located with both RHF and DFT methods. The geometries and pathways are summarized in Figure 2, and relative energies obtained with different methods are given in Table 1.

RHF/6-31G* and RB3LYP/6-31G* calculations predict similar geometries for each transition structure. Indeed, B3LYP/6-31G*//RHF/6-31G* energies are nearly the same as those obtained from full B3LYP/6-31G* optimizations. This demonstrates that electron correlation, which is included in the DFT calculations, has little effect on the geometries of the transition structures. With different methods, the (2+2) ΔE^\ddagger is relatively constant at 14–21 kcal/mol, but there are large differences in the ΔE^\ddagger values computed for the (3+2) mechanism. Correlated methods predict ΔE^\ddagger values of 12–29 kcal/mol for this pathway, and RHF/6-31G* calculations give a ΔE^\ddagger of 53 kcal/mol. The $\Delta\Delta E^\ddagger$ for the (2+2) and (3+2) pathways drops from 31 kcal/mol (favoring the (2+2) pathway) at the RHF level to 5 kcal/mol at the B3LYP/6-31G* level. Since two SO double bonds

(13) (a) Wong, M. W.; Frisch, M. J.; Wiberg, K. B. *J. Am. Chem. Soc.* **1991**, *113*, 4776 and references therein. (b) Wong, M. W.; Wiberg, K. B.; Frisch, M. J. *J. Comput. Chem.* **1995**, *16*, 385 and references therein.

(14) SPARTAN version 4.0; Wavefunction, Inc.: Irvine, CA, 1995.

(15) (a) Hay, P. J.; Wadt, W. R. *J. Chem. Phys.* **1985**, *82*, 270. (b) Hay, P. J.; Wadt, W. R. *J. Chem. Phys.* **1985**, *82*, 299.

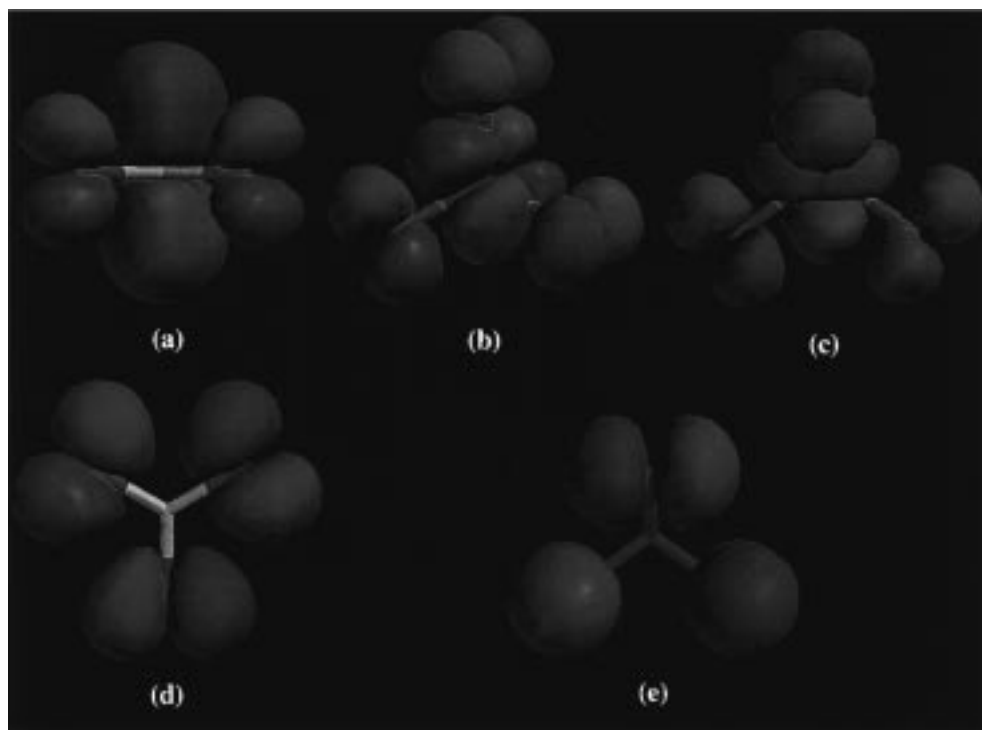


Figure 3. MO plots of the SO₃ HOMO (d) and LUMO (a), one of the three degenerate HOMOs (e), and the two degenerate LUMOs (b and c) of OsO₄.

Table 1. Relative Energies (kcal/mol) for Ground and Transition Structures of SO₃ and Ethene^a

	computational level								
	RHF ^b	MP2 ^c	MP3 ^c	MP4D ^c	MP4DQ ^c	MP4SDQ ^c	QCISD ^c	QCISD(T) ^c	B3LYP ^b
SO ₃ + ethene	0.0	0.0	0.0	0.0	0.0	0.0	0.0	0.0	0.0
SO ₃ + ethene (2+2) TS (4)	+21.2	+18.0	+20.1	+20.7	+20.7	+18.3	+17.3	+16.7	+13.6
sultone (5)	-26.0	-25.5	-27.4	-25.9	-26.8	-26.0	-25.6	-24.6	-23.6
sultone rearrangement TS (7)	+49.1	+42.0	+43.8	+42.8	+43.6	+38.5	+32.9	+33.3	+30.9
sulfite (8)	-43.4	-39.7	-45.0	-43.8	-44.6	-43.6	-43.4	-42.3	-41.4
SO ₃ + ethene (3+2) TS (6)	+52.5	+12.0	+25.3	+20.4	+28.7	+28.0	+27.6	+20.5	+18.5

^a The 6-31G* basis set was used throughout. ^b Full geometry optimizations. ^c Single-point energy calculations on RHF/6-31G* geometries.

are involved in the (3+2) reaction, and only one in the (2+2), the effect of electron correlation on the former is largest.

To establish the reliability of these results, RHF calculations utilizing larger basis sets and MPn/6-31G* single-point calculations were also performed. RHF/6-311+G**/RHF/6-31G* calculations predict ΔE^\ddagger values similar to the RHF/6-31G* results [+20.8 vs +21.2 kcal/mol for (2+2) and +52.2 vs +52.5 kcal/mol for (3+2)]. The MPn/6-31G* ΔE^\ddagger for the (3+2) transition structure, **6**, oscillates with perturbation order, but the QCISD(T)/6-31G* and B3LYP/6-31G* ΔE^\ddagger values are similar at 20.5 and 18.5 kcal/mol, respectively.

To examine the possibility of lower energy open-shell mechanisms for the (3+2), (2+2), and ring expansion reactions, unrestricted HF and DFT single-point calculations were performed. UHF single-point calculations (not included in Table 1) on the optimized RHF structures reduce the barrier for the (3+2) (**6**) and ring expansion (**7**) transition structures by 13.8 and 6.1 kcal/mol, respectively. The $\langle S^2 \rangle$ values of 0.75 and 0.87 indicate mixed spin states in the UHF calculations. These transition structures have large amounts of diradical character. However, this is not the case for the (2+2) structure. The energy of (2+2) transition structure **4** at the UB3LYP/6-31G**/RB3LYP/6-31G* level is identical to that obtained with the restricted wavefunction.

For some other reactions of sulfur compounds, high level ab initio calculations such as MP4SDQ/6-311+G(2df,p),¹⁶ MP2/6-311+G(d,p),¹⁷ and B3LYP/6-31+G(d)¹⁸ give more accurate results than RHF methods. The DFT ΔE^\ddagger in the present case is close to the QCISD(T) result.

The calculations at all levels show that although the (2+2) reaction is concerted, it also has appreciable zwitterionic character. In contrast, charges at the alkene carbon atoms (C1 and C2, Figure 2) evolve smoothly along the (3+2) pathway. In (3+2) transition state **6**, the charges are intermediate between those of the starting material and the product [the averages of the Mulliken charges on C1 and C2 are 0.0 (ethene) \rightarrow +0.15 (TS **6**) \rightarrow +0.28 (sulfite **8**)]. On the (2+2) pathway, the Mulliken charge on C2 is almost as high in the transition structure as in the product [Mulliken charges on C2 are 0.0 (ethene) \rightarrow +0.31 (TS **4**) \rightarrow +0.33 (sultone **5**)]. The charge on C1 is 0.0 (ethene) \rightarrow -0.07 (TS **4**) \rightarrow -0.07 (sultone **5**). The distance between C2 and O3 (2.150 Å) is longer than the forming C-S bond (2.093 Å). In fact, the CS bond is almost completely formed in the transition state (product: 1.830 Å). The asynchronicity gives an additional indication of the zwitterionic character of transition structure **4**. The dipole moment of the (2+2) transition structure is 7.5 D whereas that for (3+2)

(16) Hofmann, M.; Schleyer, P. v. R. *J. Am. Chem. Soc.* **1994**, *116*, 4947.

(17) Morokuma, K.; Muguruma, C. *J. Am. Chem. Soc.* **1994**, *116*, 10316.

(18) McKee, M. L. *J. Phys. Chem.* **1996**, *100*, 3473.

Table 2. Activation Barriers for the Reactions of SO₃ with Alkenes (kcal/mol, B3LYP/6-31G*)^a

reaction type	ethene			propene			isobutene		
(2+2) Markovnikov	13.6	(9.9)	[TS 4]	7.6	(2.5)	[TS 9]	3.0	(-3.2)	[TS 13]
(2+2) anti-Markovnikov				14.4	(10.8)	[TS 10]			
(3+2)	18.5	(18.4)	[TS 6]	18.1	(-)	[TS 11]			
				18.4	(18.3)	[TS 12]			

^a Values obtained with the SCIPCM solvation model ($\epsilon = 9.08$) are given in parentheses.

transition structure **6** is only 3.4 D. This confirms that the concerted (2+2) reaction mechanism has a large amount of zwitterionic character.

The preference for and zwitterionic character of the (2+2) transition structure can be understood from inspection of the reactant MOs, as depicted in Figure 3. The LUMO of SO₃ (Figure 3a) has a large p-orbital component on sulfur. The main interaction between the two reactants occurs between the HOMO of ethylene and the LUMO of SO₃, and this strongly favors CS bond formation.

The energy difference between the SO₃ HOMO and alkene LUMO is very large; consequently, this orbital interaction is less important, and would involve only CO bond formation since the SO₃ HOMO lacks a component on sulfur. If this orbital interaction were dominant, formation of (2+2) adduct in a single cycloaddition step would not occur, but formation of the (3+2) adduct could.

In the (2+2) transition structure (**4**, Figure 2), the HOMO is localized at the forming C1–S bond with a very small coefficient on C2. The transition state LUMO has a large coefficient on C2. This behavior fits the description of Yamaguchi *et al.*¹⁹ for symmetry-forbidden concerted cycloaddition reactions. The high polarization of one component (here SO₃) causes the LUMO to be essentially localized on sulfur and the HOMO (Figure 3d) on oxygen. Consequently, there is no crossing of orbital energy levels during the course of concerted reaction and no orbital symmetry forbiddenness for the reaction. Roberts and co-workers reached the same conclusion for the (2+2) reaction of SO₃ with alkenes on the basis of orbital correlation analyses.^{4a}

In (3+2) transition structure **6**, the HOMO of the alkene must interact with the oxygen atoms of SO₃. The SO₃ LUMO coefficients are very small on oxygen, and the HOMO-alkene/LUMO-SO₃ overlap is poor. In addition, the interaction between the alkene HOMO and the large sulfur p-orbital component of the SO₃ LUMO is repulsive, and the activation barrier is consequently higher than that of the (2+2) reaction. The substantial reduction in activation energy of the (3+2) route by inclusion of correlation energy reflects this lack of stabilizing HOMO–LUMO interactions. In such a case, transition state stabilization arises primarily from higher order interactions, not involving simple HOMO–LUMO stabilization. Because of the FMO shapes, the (3+2) reaction of SO₃ expresses the characteristics of an orbital symmetry forbidden process, while the (2+2) is like an orbital symmetry allowed process. The situation is completely different in the osmylation reaction.

The doubly degenerate LUMO of OsO₄ (Figure 3b,c) has large coefficients on the oxygen atoms and small coefficients on osmium, and the electrophilic (3+2) cycloaddition can occur readily. The apparent similarity of the reactants belies the very different chemistry observed with these compounds. B3LYP calculations clearly differentiate between the reaction pathways and give results in good accord with experiment. The OsO₄

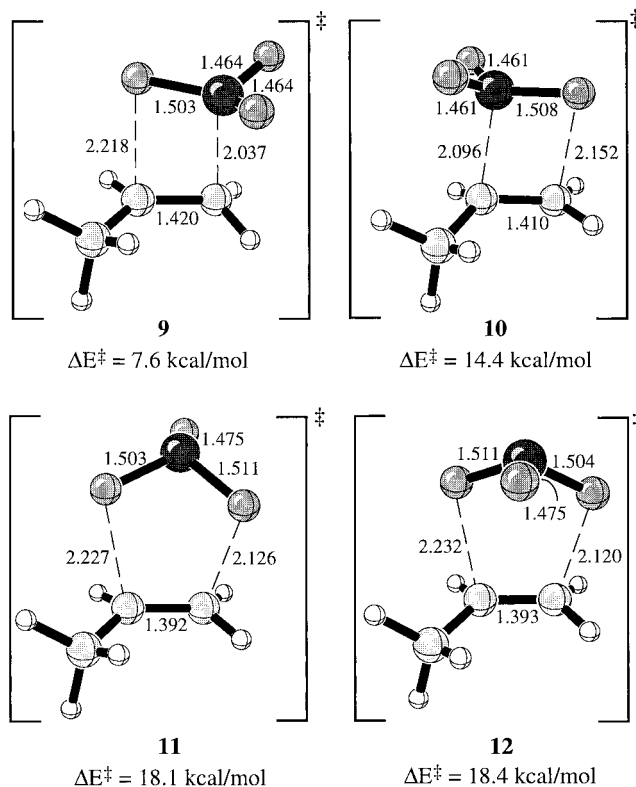


Figure 4. The (2+2) and (3+2) transition structures and activation energies (B3LYP/6-31G*) for cycloaddition reactions of SO₃ with propene. All bond lengths are in Å.

LUMO resembles that of a diene, with respect to the terminal coefficients, and both can enter into concerted cycloadditions with alkenes.

Our best calculations predict a concerted (2+2) cycloaddition mechanism for the reaction of ethene with SO₃ with a ΔE[‡] of 14–17 kcal/mol. The ΔE[‡] for the (3+2) cycloaddition pathway is about 5 kcal/mol higher. Since the (2+2) transition structure is highly polar, it should be stabilized more effectively by polar solvents than the (3+2) transition structure. This prediction is supported by calculations simulating solvation with the SCIPCM model.¹³ Using the dielectric constant of dichloromethane, 9.08, the relative energy of (2+2) transition structure **4** is lowered by 3.7 kcal/mol, whereas the activation barrier of the (3+2) reaction remains essentially unchanged (Table 2).

Sulfite **8** is considerably more stable than sultone **5** at all levels of theory (Table 1). The energy difference is 18 kcal/mol at the B3LYP/6-31G* level. Despite this, the ΔE[‡] for the 1,2 shift converting the sultone to the sulfite is large—55 kcal/mol at the B3LYP level.

The observed Markovnikov addition of SO₃ to substituted olefins (with respect to the position of the sulfur atom as electrophile) can also be explained by the zwitterionic character of the transition structure.

SO₃ Plus Propene and Isobutene. The ΔE[‡] for the (3+2) mechanism of the SO₃/propene cycloaddition (**11**, Figure 4) is about the same as that for the SO₃/ethene (3+2) mechanism

(19) (a) Yamaguchi, K.; Fueno, T.; Fukutome, H. *Chem. Phys. Lett.* **1973**, 22, 461. (b) Yamaguchi, K.; Fueno, T.; Fukutome, H. *Chem. Phys. Lett.* **1973**, 22, 466.

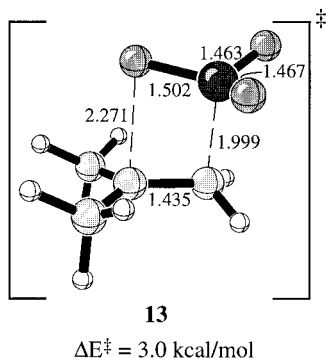


Figure 5. Markovnikov (2+2) transition structure and activation energy (B3LYP/6-31G*) for the cycloaddition reaction of SO₃ and isobutene. All bond lengths are in Å.

(6). Thus, SO₃ is not particularly electrophilic when reacting by the (3+2) route (Table 2). For the (2+2) cycloadditions of propene, when the methyl group is in the anti-Markovnikov position (**10**), the ΔE^\ddagger increases compared to that for the ethene reaction (14.4 kcal/mol (**10**) vs 13.6 kcal/mol (**4**)). When the methyl group is located at the partially positively charged carbon atom in **9**, the transition structure is stabilized by 6 kcal/mol compared to the reaction with ethene (**4**). The $\Delta\Delta E^\ddagger$ of 7 kcal/mol favoring formation of regioisomer **9** over **10** makes the Markovnikov adduct the only observable product. With the SCIPCM solvent model the preference for Markovnikov addition increases to over 8 kcal/mol.

The second methyl group in isobutene (**13**, Figure 5) lowers the ΔE^\ddagger by an additional 4.6 kcal/mol. This trend parallels that observed for the heats of formation of the corresponding cations in the gas phase.²⁰ The energy difference between the *n*-propyl cation (211 kcal/mol) and the isopropyl cation (191 kcal/mol)

(20) Lias, S. G.; Bartmess, J. E.; Liebman, J. F.; Holmes, J. L.; Levin, R. D.; Mallard, W. G. *J. Phys. Chem. Ref. Data* **1988**, *17*, Suppl. 1.

is about three times as large as the energy difference between transition states **9** and **10**. The isobutyl cation (199 kcal/mol) and the *tert*-butyl cation (166 kcal/mol) differ by 33 kcal/mol, which is about 3 times the difference between the activation energies for reactions involving ethene (**4**) and propene (**10**). Although zwitterionic character is substantial, it is incomplete in these transition states.

Conclusions

The cycloaddition reactions of SO₃ with olefins follow a concerted, but decidedly asynchronous, (2+2) reaction pathway involving transition structures with substantial zwitterionic character. Regioselectivity follows Markovnikov's Rule. Due to the polar character of the transition structure, the (2+2) activation barrier is predicted to be lowered substantially by polar solvents, while the experimentally unobserved (3+2) pathway is relatively unaffected. These results provide another example of the reliability and validity of DFT calculations with the B3LYP functional, and demonstrate that this method does not incorrectly favor (3+2) over (2+2) cycloaddition mechanisms. The contrast between mechanisms and products of SO₃ and OsO₄ reactions is readily explained in terms of frontier molecular orbital theory.

Acknowledgment. We wish to dedicate this paper to Kenichi Fukui, recently deceased, who showed how to interpret chemical reactivity with frontier molecular orbital theory. We thank Professors K. B. Sharpless and A. K. Rappé for suggesting this study and for helpful discussions. We are grateful to the National Science Foundation for financial support of this research and to the UCLA Office of Academic Computing for computer time and facilities. J.H. thanks the Alexander von Humboldt Foundation for a Feodor Lynen fellowship. We thank Amy Keating and Dr. Thomas Strassner for helpful advice.

JA974236N